Solvation and Axial Ligation Properties of (2,3,7,8,12,13,-17,18-Octabromo-5,10,15,20-tetraphenylporphyrinato)zinc(II) †

Puttaih Bhyrappa,[a] Varadachari Krishnan *[,a,b] and Munirathinam Nethaji[a]
[a] *Department of Inorganic and Physical Chemistry, Indian Institute of Science, Bangalore 560 012, India*
[b] *Jawaharlal Nehru Centre for Advanced Scientific Research, Indian Institute of Science Campus, Bangalore 560 012, India*

The solvation of (2,3,7,8,12,13,17,18-octabromo-5,10,15,20-tetraphenylporphyrinato)zinc(II) [Zn(obtpp)], in twelve different solvents results in large red shifts of the B and Q bands of the porphyrin accompanied by enhanced absorbance ratios of the Q bands. These observations are ascribed to the destabilisation of the highest occupied molecular orbital a_{2u} of the porphyrin arising from a flow of charge from the axial ligand to the porphyrin ring through the zinc(II) ion. The binding constants of adducts of [Zn(obtpp)] with neutral bases have been found to be an order of magnitude greater than those observed for the corresponding adducts of (5,10,15,20-tetraphenylporphyrinato)-zinc and vary in the order piperidine > imidazole > pyridine > 3-methylpyridine > pyridine-3-carbaldehyde. The enhanced binding constants and large spectral shifts are interpreted in terms of the electrophilicity of [Zn(obtpp)] induced by the electron-withdrawing bromine substituents in the porphyrin core. The structure of [Zn(obtpp)(PrCN)$_2$] has been determined; it reveals six-co-ordinated zinc(II) with two long Zn–N distances [2.51(4), 2.59(3) Å]. The porphyrin is non-planar and displays a saddle-shaped conformation.

Metalloporphyrins provide the possibility to study a wide range of metal-ion co-ordination behaviour. Those containing higher-valent metal ions (Mn^{III}, Fe^{III}, Co^{III} and Sn^{IV}) exhibit pronounced changes in the optical absorption spectra with varying nature of the axial ligands.[1] This has been interpreted in terms of in- and out-of-plane bonding of the metalloporphyrins and the extent to which the axial ligand changes the M–N σ bonding. Detailed studies on the solvation and axial ligation properties of (5,10,15,20-tetraphenylporphyrinato)zinc(II) [Zn(tpp)] have been reported.[2–4] These investigations have shed light on the manner by which axial ligands induce changes in the optical absorption features of the metalloporphyrins. It is of interest to investigate the effect of different substituents at the peripheral positions of the porphyrin on the axial ligation behaviour of the central metal ions.

Recently we reported a new class of metalloporphyrins, octabromotetraphenylporphyrins, and demonstrated that the bromine substituents at the β-pyrrole carbons of the porphyrin induce electrophilicity in the π ring.[5] This is evidenced from the large red shifts of the Soret and Q bands relative to those observed for the unsubstituted tetraphenylporphyrins and the ease of the bromoporphyrins to undergo one-electron ring reductions. These interesting features led us to investigate the solvation and axial ligation properties of these porphyrins.

We report here the optical absorption and ^{1}H NMR spectral features of (2,3,7,8,12,13,17,18-octabromo-5,10,15,20-tetraphenylporphyrinato)zinc [Zn(obtpp)] in different solvents and elucidate the axial ligation properties with different donors, piperidine, imidazole, pyridine, 3-methylpyridine and pyridine-3-carbaldehyde. This metalloporphyrin was chosen because of its ease of solubility in different solvents relative to other metal derivatives. The extensive data available on the axial ligation/solvation properties of the corresponding unsubstituted derivative [Zn(tpp)] permit a comparison of the properties with those of [Zn(obtpp)]. This has enabled us to isolate the effects induced by the bromine substituents at the porphyrin macrocycle on the solvation/ligation behaviour of the central metal ion. The crystal structure of one of the solvates was determined and has been helpful in the analysis of the axial ligation features.

† *Supplementary data available:* see Instructions for Authors, *J. Chem. Soc., Dalton Trans.*, 1993, Issue 1, pp. xxiii–xxviii.

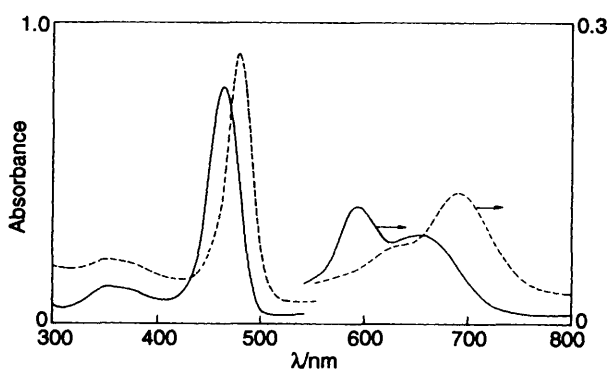

Fig. 1 Optical absorption spectrum of [Zn(obtpp)] in heptane (——) and Me_2SO (– – – –) at 298 K

Results

The optical absorption spectra of [Zn(obtpp)] in two representative solvents are shown in Fig. 1. The oscillator strength (f) of the B and Q transitions was calculated from the expression [6] $f = 4.33 \times 10^{-9} \varepsilon \nu_{\frac{1}{2}}$ where ε is the molar absorption coefficient in $dm^3\ mol^{-1}\ cm^{-1}$ and $\nu_{\frac{1}{2}}$ is the full width at half maximum (f.w.h.m.) in cm^{-1}. The data obtained in different solvents are given in Table 1. The optical absorption parameters that are of interest are the positions of the absorption bands, the oscillator strengths of the transitions and the ratios of the intensities of the two visible bands, Q(0,0) and Q(1,0), in increasing order of energies.

A perusal of Table 1 reveals the following. (*i*) The B (Soret) and Q transitions are shifted to the red region in different solvents relative to what is observed in heptane; the magnitude of the shifts are larger for the Q than for the B band. (*ii*) There is

Table 1 Optical absorption spectral data for [Zn(obtpp)] in different solvents * at 298 K

		λ/nm		
No.	Solvent	B bands	Q(1,0)	Q(0,0)
1	Heptane	352 (4.50), 465 (5.22) [1.10]	592 (4.05)	649 (3.90) [0.077]
2	$CHCl_3$	354 (4.60), 466 (5.41) [1.39]	598 (4.11)	653 (4.02) [0.08]
3	CCl_4	355 (4.35), 468 (5.34) [1.21]	598 (4.05)	654 (3.96) [0.065]
4	CH_2Cl_2	351 (4.62), 466 (5.43) [1.51]	603 (4.04)	658 (4.05) [0.077]
5	Toluene	355 (4.50), 472 (5.37)	603 (4.04)	658 (3.99) [0.0588]
6	MeOH	351 (4.41), 468 (5.38) [1.20]	615 (3.94)	670 (4.09) [0.068]
7	MeCN	354 (4.45), 473 (5.31) [1.07]	623 (3.89)	680 (4.09) [0.077]
8	BuCN	352 (4.46), 474 (5.27) [1.06]	626 (3.92)	684 (4.13) [0.092]
9	thf	354 (4.47), 473 (5.36) [1.07]	617 (3.94)	675 (4.11) [0.077]
10	dmf	354 (4.52), 477 (5.37) [1.23]	630 (3.91)	684 (4.19) [0.091]
11	Me_2SO	354 (4.37), 481 (5.34) [1.10]	642 (3.91)	693 (4.20) [0.105]
12	Pyridine	371 (4.45), 481 (5.38) [1.13]	636 (3.94)	689 (4.21) [0.084]

* The values in parentheses refer to log ε values while the oscillator strength is given in square brackets.

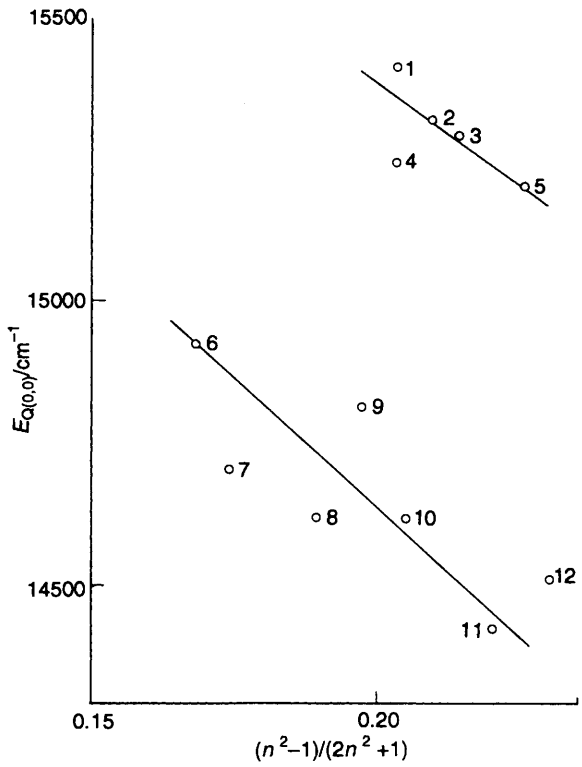

Fig. 2 Plot of the energy of the longest-wavelength band, $E_{Q(0,0)}$, of [Zn(obtpp)] *versus* the polarisability parameter of different solvents. The numbers denote the solvents in Table 1

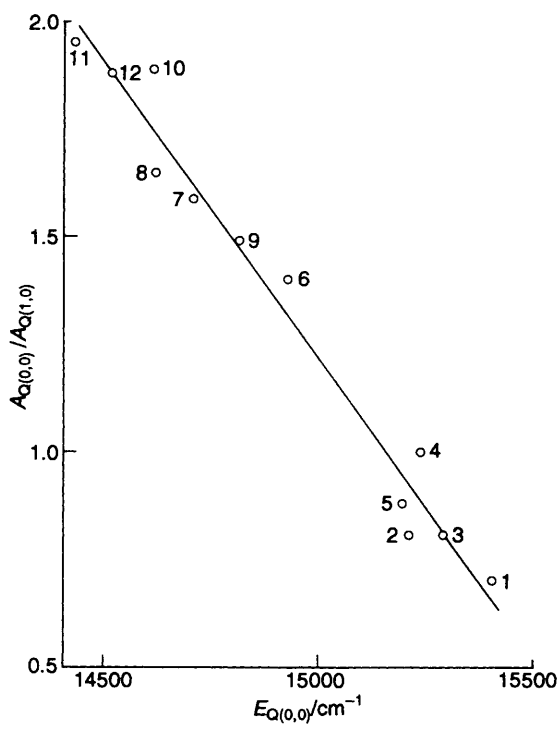

Fig. 3 Plot of the absorbance ratio against the energy of the longest-wavelength band of [Zn(obtpp)] in different solvents. The numbers denote the solvents in Table 1

a marginal increase in the log ε values of the B band in different solvents relative to what is found in heptane, whereas the intensities of the Q bands exhibit different trends with varying solvent polarity. Thus, the Q(0,0) band exhibits a marginal increase in log ε while the Q(1,0) band shows a decrease in log ε relative to what is observed in heptane. However, the absorbance ratio $A_{Q(0,0)}/A_{Q(1,0)}$ increases with increase in solvent polarity. (*iii*) The *f* values are found to be larger in polar solvents relative to non-polar solvents. (*iv*) The magnitude of the red shift of the Q transitions is two to three times larger for [Zn(obtpp)] while the shift in the B band is not significantly different from those observed for [Zn(tpp)].[2] However, the ratio of the absorbances of the Q(0,0) to Q(1,0) bands of [Zn(obtpp)] is three to six times larger than those reported for [Zn(tpp)].

These observations are rationalised in terms of the solvation/axial ligation of [Zn(obtpp)]. In order to isolate the effect induced by solvation, plots of the energy of the longest-wavelength band $E_{Q(0,0)}$ *versus* the polarisability parameter $(n^2 - 1)/(2n^2 + 1)$, where n is the refractive index, were constructed (Fig. 2). It is seen that solvents are divided into two groups around straight lines of different slopes, the polar solvents have a larger slope (*ca.* 1.0) than that of the non-polar solvents (*ca.* 0.6). This is interpreted in terms of co-ordinative (polar) and weak (non-polar solvation) interaction of the different solvents with [Zn(obtpp)]. The solvents which fall on the line of smaller slope have donor numbers of nearly zero, while the other group have higher donor numbers.[7] A plot of the absorbance ratio $A_{Q(0,0)}/A_{Q(1,0)}$ against the energy of the longest-wavelength band $E_{Q(0,0)}$ observed in different solvents (Fig. 3) is nearly linear. In the polar and co-ordinative solvents larger red shifts and enhanced absorbance ratios relative to other non-polar solvents are observed. The absence of any break in Fig. 3 in contrast to Fig. 2 indicates that the magnitude of the red shift and the change in the absorbance ratio arise from both solvation and axial ligation properties.

The equilibrium constants for the complexation of metal octabromotetraphenylporphyrins with several neutral bases have been measured. Typical absorption spectra of [Zn(obtpp)] in toluene on addition of increasing amounts of pyridine are shown in Fig. 4. The decrease in the absorbance at 603 nm and the increase at 658 nm were monitored for the evaluation of the equilibrium constant. The stoichiometry of the complexes in solution as determined by a Hill plot[8] suggests that the

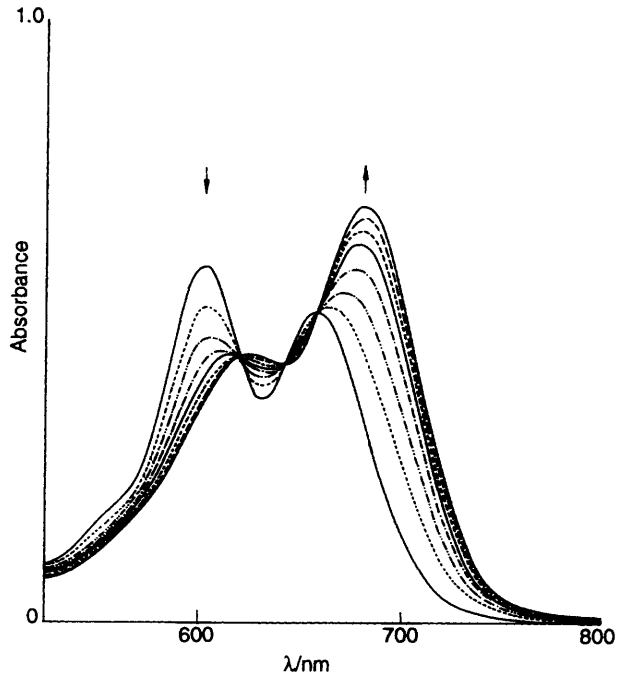

Fig. 4 Optical absorption spectra of [Zn(obtpp)] (5×10^{-5} mol dm^{-3}) in toluene on successive additions of pyridine (1.0×10^{-4}–1.0×10^{-2} mol dm^{-3}) at 298 K

predominant species have 1 : 1 stoichiometry indicating five-co-ordination. The equilibrium constants (K) determined using the method of Miller and Dorough [9] are given in Table 2 along with corresponding values for [Zn(tpp)].[10,11] It is seen that the K values for complexation of [Zn(obtpp)] are an order of magnitude greater than those of [Zn(tpp)] indicating the electrophilicity of [Zn(obtpp)] as a consequence of the bromine substituents at the peripheral positions of the porphyrin. The pK values of the bases bear a linear relationship with log K indicating their co-ordination to the [Zn(obtpp)].

The base co-ordination to [Zn(obtpp)] as studied by ^{1}H NMR spectroscopy yielded interesting results. The spectra of the different adducts revealed high-field shifts (Fig. 5) for the protons of the co-ordinated bases similar to those observed for the base complexation by [Zn(tpp)].[12] These shifts represent weighted averages of the chemical shifts of the protons of the free base and of the base co-ordinated by [Zn(obtpp)] in solution. That the chemical shift of the base protons arises essentially from the five-co-ordinated [Zn(obtpp)] can be rationalised as follows. Addition of less than 1 equivalent of base to an equivalent amount of [Zn(obtpp)] in solution results in a high-field shift of the resonance of the base protons, while addition of more than 1 equivalent of base shifts the resonance to lower fields indicating exchange averaging. In view of the large magnitude of the equilibrium constants of the base complexes of [Zn(obtpp)], the chemical shifts observed for the base protons in solutions containing less than 1 equivalent of base truly represent the shifts of the five-co-ordinated [Zn(obtpp)] since under these conditions no free uncomplexed base can exist in solution. Moreover, the ^{1}H NMR spectra of solutions containing [Zn(obtpp)] and 2 equivalents of base measured at low temperature (−50 °C) showed no line broadening or any evidence of slowing of the exchange rate. The position of the exchange-averaged base proton resonance remained unchanged with increase or decrease in temperature, indicating that the dominant species in solution is the five-co-ordinated base complex of [Zn(obtpp)]. It is of note that the magnitude of the high-field shifts of the base protons in the [Zn(obtpp)] complex is found to be larger than those observed for the corresponding base complex of [Zn(tpp)] suggesting an electrophilic nature of [Zn(obtpp)].

Table 2 Equilibrium constants for axial ligation of bases with [Zn(obtpp)] and [Zn(tpp)] in toluene at 298 K

	log K		
Base	[Zn(obtpp)]*	[Zn(tpp)]	pK
Piperidine	6.16	5.05	11.10
Imidazole	5.84	4.73	6.65
3-Methylpyridine	5.24	3.81	5.79
Pyridine	4.84	3.78	5.29
Pyridine-3-carbaldehyde	4.00	3.24	4.70
Dimethyl sulfoxide	4.12	3.60	

* Uncertainty ± 8%.

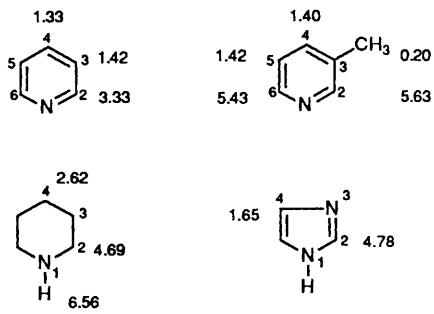

Fig. 5 The shifts of proton resonances of the different bases on complexation with [Zn(obtpp)] in $CDCl_3$

Crystal Structure of [Zn(obtpp)(PrCN)$_2$] **1**.—Complex **1** crystallised in the triclinic system with two molecules in the unit cell and is isomorphous with the six-co-ordinate structure of [Zn(tpp)(thf)$_2$][13] (thf = tetrahydrofuran). The atomic co-ordinates are given in Table 3 and selected bond lengths and angles of the porphyrin skeleton including the axially co-ordinated ligand molecules are given in Table 4. Fig. 6 depicts the atom numbering scheme, and an ORTEP diagram[14] is shown in Fig. 7. The structure bears close similarity with those of the recently investigated 2,3,7,8,12,13,17,18-octabromo-5,10,15,20-tetramesitylporphyrin and its nickel(II) complex[15] and (2,3,7,8,12,13,17,18-octaalkyl-5,10,15,20-tetraphenylporphyrinato)zinc(II) derivatives.[16] The zinc ion is tetragonally distorted with two axially coordinated butyronitrile molecules and four equatorial nitrogen atoms from the porphyrin ring. It is of note that the zinc deviates from the least-squares plane of the porphyrin by 0.058 Å, indicating expansion of the porphyrin core. The *meso*-phenyl and the pyrrole rings are planar within the limit of 0.01 Å. The C–C bond lengths of the phenyl groups are in the range 1.36–1.45 Å and exhibit no significant deviation from normal aromatic systems. It is noteworthy that the phenyl rings are rotated by 56.3–58.8° from the mean porphyrin plane in contrast to 75–80° reported for the [Zn(tpp)] derivative.[17] The *meso*-carbon to phenyl carbon bond distance is found to be 1.49–1.51 Å characteristic of σ bonding and indicating the absence of electronic conjugation of the phenyl groups with the porphyrin π system. Interestingly, adjacent pyrrole rings are tilted by an angle of 32.2–35.2° and the opposite pyrrole rings deviate from the least-squares plane by 48.6–50.2°. The pyrrole rings are tilted to prevent the repulsive interactions among the bromine substituents and between the bromine and the *meso*-phenyl groups, resulting in an increase in C(3)–C(4)–C(5) angle and decreases in the N(1)–C(4)–C(5) and Zn–N(1)–C(4) angles (Table 4). It is of note that the bromine atoms at the pyrrole rings are non-equivalent since adjacent bromine atoms of a given ring deviate by 0.59 Å. However, the bromine atoms on pyrrole rings I and III are positioned above, while those on the other two II and IV are situated below the least-squares plane of the porphyrin ring.

Table 3 Atomic positional parameters of non-hydrogen atoms of [Zn(obtpp)(PrCN)$_2$] with estimated standard deviations (e.s.d.s) in parentheses

Atom	x	y	z	Atom	x	y	z
Zn	−0.1469(2)	0.1796(2)	0.7441(3)	Br(5)	0.2549(1)	0.0604(2)	0.8496(2)
Br(1)	−0.4709(2)	0.4093(2)	0.8777(2)	Br(6)	0.2833(1)	0.3142(2)	0.8976(2)
Br(2)	−0.4736(2)	0.1974(2)	0.9268(2)	C(11)	0.0435(10)	0.0873(20)	0.7572(20)
C(1)	−0.3254(12)	0.2955(13)	0.7720(15)	C(12)	0.1495(10)	0.1274(10)	0.8061(20)
C(2)	−0.4000(14)	0.2982(14)	0.8219(16)	C(13)	0.1668(10)	0.2291(10)	0.8231(10)
C(3)	−0.4006(12)	0.2160(14)	0.8450(16)	C(14)	0.0659(10)	0.2499(10)	0.7759(20)
C(4)	−0.3332(11)	0.1482(14)	0.7956(15)	N(3)	−0.0033(10)	0.1636(10)	0.7432(10)
N(1)	−0.2827(10)	0.2037(11)	0.7609(12)	C(15)	0.0446(10)	0.3372(10)	0.7588(10)
C(5)	−0.3214(12)	0.0455(14)	0.7782(15)	C(151)	0.1303(20)	0.4108(20)	0.7715(20)
C(51)	−0.4004(12)	−0.0123(14)	0.7927(16)	C(152)	0.1518(10)	0.5115(10)	0.8655(20)
C(52)	−0.4932(13)	−0.0463(14)	0.7170(17)	C(153)	0.2378(20)	0.5789(20)	0.8780(20)
C(53)	−0.5704(16)	−0.1001(15)	0.7328(18)	C(154)	0.2899(20)	0.5452(20)	0.8034(20)
C(54)	−0.5432(15)	−0.1263(16)	0.8193(18)	C(155)	0.2627(10)	0.4472(20)	0.7168(20)
C(55)	−0.4518(15)	−0.0900(15)	0.8944(17)	C(156)	0.1829(10)	0.3737(10)	0.6969(20)
C(56)	−0.3748(12)	−0.0356(15)	0.8822(15)	Br(7)	−0.0136(1)	0.4926(2)	0.6218(2)
N(S5)	−0.0653(25)	0.2679(20)	0.9547(20)	Br(8)	−0.2612(2)	0.4877(2)	0.5793(2)
C(1S5)	0.1026(29)	0.1296(33)	1.0509(32)	C(16)	−0.0521(10)	0.3595(10)	0.7243(20)
C(2S5)	0.1384(19)	0.2311(29)	1.1007(21)	C(17)	−0.0834(10)	0.4210(10)	0.6688(20)
C(3S5)	0.0669(30)	0.3146(31)	1.1087(31)	C(18)	−0.1845(10)	0.4272(10)	0.6586(20)
C(4S5)	−0.0353(37)	0.2453(38)	1.0147(39)	N(4)	−0.1311(10)	0.3167(10)	0.7394(10)
Br(3)	−0.3437(2)	−0.2311(2)	0.6556(2)	C(19)	−0.2122(10)	0.3621(10)	0.7031(10)
Br(4)	−0.1277(2)	−0.2714(2)	0.6012(2)	C(20)	−0.3022(10)	0.3616(10)	0.7299(10)
C(6)	−0.2487(12)	−0.0079(14)	0.7424(14)	C(201)	−0.3703(10)	0.4338(10)	0.7162(10)
C(7)	−0.2457(12)	−0.1211(13)	0.6958(14)	C(202)	−0.3451(10)	0.5420(10)	0.7902(10)
N(2)	−0.1606(9)	0.0419(10)	0.7502(12)	C(203)	−0.4076(20)	0.6144(20)	0.7824(20)
C(8)	−0.1582(15)	−0.1393(15)	0.6753(16)	C(204)	−0.4936(20)	0.5784(20)	0.6917(20)
C(9)	−0.1031(12)	−0.0334(14)	0.7154(15)	C(205)	−0.5206(20)	0.4700(20)	0.6172(20)
C(10)	−0.0027(12)	−0.0124(13)	0.7244(14)	C(206)	−0.4559(10)	0.3968(10)	0.6313(10)
C(101)	0.0605(13)	−0.1000(14)	0.7082(17)	C(1S14)	−0.3532(30)	−0.1648(30)	0.4004(30)
C(102)	0.0855(15)	−0.1394(16)	0.7828(19)	C(2S14)	−0.4338(20)	−0.1125(20)	0.4521(20)
C(103)	0.1479(19)	−0.2269(18)	0.7575(26)	C(3S14)	−0.2960(30)	−0.1074(30)	0.3793(30)
C(104)	0.1734(16)	−0.2647(18)	0.6685(22)	C(4S14)	−0.2481(20)	0.0025(30)	0.4739(30)
C(105)	0.1528(20)	−0.2200(20)	0.5967(20)	N(S14)	−0.2247(30)	0.0756(30)	0.5406(30)
C(106)	0.0917(10)	−0.1376(10)	0.6170(20)				

Table 4 Selected bond lengths (Å) and angles (°) with e.s.d.s in parentheses

Zn–N(1)	2.03(2)	N(1)–Zn–N(S5)	91.2(1)
Zn–N(S5)	2.59(3)	N(1)–Zn–N(2)	90.6(1)
Zn–N(2)	2.02(2)	N(1)–Zn–N(3)	174.5(1)
Zn–N(3)	2.06(2)	N(1)–Zn–N(S14)	89.9(1)
Zn–N(4)	2.00(2)	N(S5)–Zn–N(S14)	173.9(1)
Zn–N(S14)	2.51(4)	C(1)–N(1)–C(4)	108.8(2)
C(1)–C(2)	1.43(3)	C(2)–C(1)–N(1)	106.5(2)
C(1)–N(1)	1.41(2)		
C(2)–C(3)	1.35(3)	C(1)–C(2)–C(3)	109.9(2)
C(3)–C(4)	1.41(3)	C(2)–C(3)–Br(2)	124.8(2)
C(4)–C(5)	1.40(3)	C(3)–C(2)–Br(1)	121.2(2)
C(5)–C(51)	1.50(3)	C(3)–C(4)–C(5)	129.6(2)
C(2)–Br(1)	1.88(2)	N(1)–C(4)–C(5)	123.5(2)
C(3)–Br(2)	1.86(2)	Zn–N(1)–C(4)	123.6(1)

These structural features indicate that the porphyrin skeleton of complex **1** exhibits a saddle type of geometry.[15,16,18]

Discussion

A quantitative understanding of the optical absorption spectral features of [Zn(obtpp)] in different solvents is possible from the four-orbital approach of Gouterman.[19] The energy states of the highest-occupied molecular orbital (HOMO) (a_{1u} and a_{2u}) and the lowest unoccupied molecular orbital (LUMO) (e_g π^*) of the porphyrin system are shown in Fig. 8. The parameters defining the energies of the excited-state molecular orbitals are the matrix elements A_{1g} (energy separation between a_{1u} and a_{2u} orbitals), A_{1g}' (average energy of B and Q bands), the configuration interaction (c.i.) element A_{1g}'' and r/R, the ratio of the transition dipoles of one-electron states. Earlier we showed[5] that the presence of electron-withdrawing bromine substituents

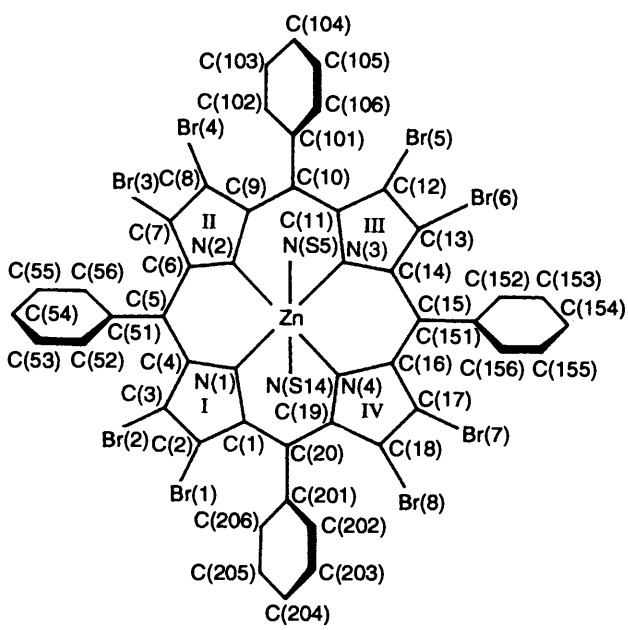

Fig. 6 Atomic numbering scheme for the [Zn(obtpp)(PrCN)$_2$] complex. The carbon atoms of the solvent molecules are not shown

at the pyrrole carbons results in enhanced conjugation of the porphyrin ring leading to delocalisation of the ring charge and decrease in the magnitude of A_{1g}''. The general effect is to decrease the separation of B and Q states and stabilisation of e_g (π^*) orbitals. The observed red shift of the B and Q transitions and increased absorbance ratio of the Q bands of [Zn(obtpp)] with increasing solvent polarity can be interpreted as follows.

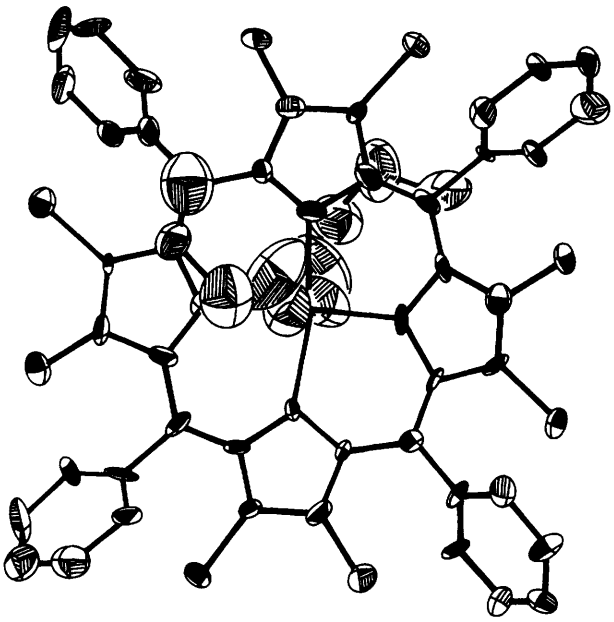

Fig. 7 An ORTEP diagram of [Zn(obtpp)(PrCN)$_2$] with thermal ellipsoids, showing 50% probability

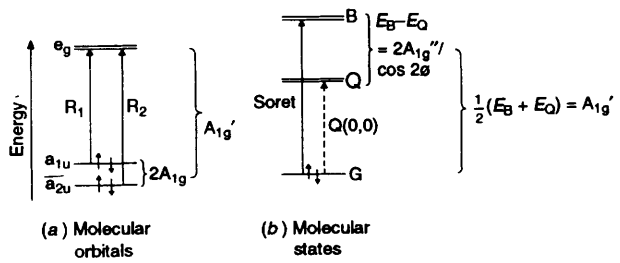

Fig. 8 Diagram showing the parameters of the four-orbital model. Here tan 2ϕ is defined as the ratio of A_{1g} and A_{1g}''

The ligation of solvent molecules to zinc(II) leads to a flow of charge from the ligand to the octabromoporphyrin ring through the central metal ion, thereby destabilising the HOMO a_{2u} relative to a_{1u}. The perturbation of the a_{2u} orbital is expected to be greater since this orbital has electron density at the imino nitrogens while a_{1u} has no electron density at these nitrogen centres. In addition to this destabilisation, the configuration-interaction matrix element is also expected to change in the solvated complex of [Zn(obtpp)] owing to decreased electron–electron repulsion.[5] This is evidenced from the energy separation of the B and Q bands, $E_B - E_Q$. Thus in weakly co-ordinating non-polar solvents (1–4 in Table 1) the average value of $E_B - E_Q$ is found to be 6110 cm^{-1}, while an increase in this value (to 6400 cm^{-1}) is found for the polar co-ordinative solvents (5–12 in Table 1). It is of interest that the $E_B - E_Q$ values found for [Zn(obtpp)] in different solvents are smaller than corresponding ones for [Zn(tpp)]. This is explained in terms of the decreased c.i. matrix element (5050 cm^{-1}) relative to [Zn(tpp)] solvates (6330 cm^{-1}). An alternative interpretation for the observed red shifts of the B and Q bands and enhanced absorbance ratio of the Q bands of the [Zn(obtpp)] solvates lies in the relative disposition of the zinc(II) ion in the porphyrin. Co-ordination of solvent/base molecules to zinc(II) in [Zn(obtpp)] can displace the metal ion in or out of the porphyrin plane depending on the relative basicity of the ligands, thereby decreasing the molecular symmetry of the complex (away from D_{4h} symmetry). This would result in a lifting of the degeneracy of the electronic ground state of the complex. The crystal structure of [Zn(obtpp)(PrCN)$_2$] has been useful in this regard.

Interestingly, the butyronitrile solvate has the composition [Zn(obtpp)(PrCN)$_2$]. The two solvent molecules are co-ordinated with Zn–N 2.51(4), 2.59(3) Å. Among the known structures of zinc(II) porphyrins with axially co-ordinated ligands, the present solvate has the longest Zn–N distance, indicating weak co-ordination of the solvent. Thus, the five-co-ordinated (octamethyltetraphenylporphyrinato)zinc(II) pyridine adduct[16] possessing a ruffled structure has Zn–N 2.14(5) Å and the corresponding adduct of (5,10,15,20-tetrakis(4-pyridyl)-porphyrinato)zinc(II)[20] has Zn–N 2.143(5) Å. The only known disolvate of [Zn(tpp)] is the adduct of tetrahydrofuran[13] which has Zn–O 2.33(2) Å. The longer distances of Zn–N in the disolvate of [Zn(obtpp)] indicates the absence of repulsive Van der Waals interaction between axial and equatorially co-ordinated nitrogen atoms. The angle N(S5)–Zn–N(S14) is 173.9°. The nitrogen atoms of the disordered butyronitrile molecules have different conformations positioned normal to the porphyrin plane with varying C–C bond lengths (1.33–1.65 Å). The unit cell of the disolvate revealed that the centre-to-centre distance between the two molecules is greater than 7.0 Å and the closest distance between the two identical phenyl groups of the two molecules is more than 3.50 Å indicating absence of intermolecular interaction. This suggests that the distortion of the porphyrin core is not due to any interaction between the two molecules in the unit cell. The structural data seem to be consistent with the view that effects of solvation/axial co-ordination arise predominantly from electronic rather than steric considerations. This is borne out by the fact that the 'saddle' conformation of the porphyrinate core arises from the substitution at the pyrrole carbons and subsequent solvent co-ordination to the metal centre does not alter the structure in any perceptible manner. It should be noted that in solution the zinc(II) is five-co-ordinated in the presence of solvents/bases whereas it is six-co-ordinated in the solid state. We tend to believe that the complexation of [Zn(obtpp)] in solution initially proceeds through the formation of a five-co-ordinated complex [Zn(obtpp)L] leading finally to a six-co-ordinated species, [Zn(obtpp)L$_2$]. It is likely that both five- and six-co-ordinated zinc(II) species exist in solution with the five-co-ordinated [Zn(obtpp)] exhibiting a large stability constant relative to [Zn(obtpp)L$_2$], similar to the observation of Giraudeau *et al.*[21] It has been shown that (tetracyano-tetraphenylporphyrinato)nickel(II) binds one pyridine with a stability constant of 110 cm^3 mol^{-1} while the bis(pyridine) adduct has a much lower binding constant (7.0 dm^3 mol^{-1}). The stability constants of [Zn(obtpp)] with different bases decrease in the order piperidine > imidazole > pyridine > 3-methylpyridine > pyridine-3-carbaldehyde. The basicities of these ligands bear a direct relationship with the log K values. The enhanced magnitude of the stability constants of the [Zn(obtpp)] complexes relative to the corresponding [Zn(tpp)] complexes is ascribed to enhanced electrophilicity of the octabromotetraphenylporphyrin ring induced by the bromine substituents. The present study affords a novel approach to inducing stronger binding of bases to a metalloporphyrin without changing the nature of the metal ion.

Experimental

All the solvents employed were spectral grade. Piperidine and 3-methylpyridine (Ranbaxy Labs., India) were refluxed over KOH pellets for 6 h, distilled and stored over molecular sieves. Imidazole obtained from BDH (India) was used without further purification. Pyridine-3-carbaldehyde (Aldrich, USA) was used as received. (2,3,7,8,12,13,17,18-octabromo-5,10,15,20-tetraphenylporphyrinato)zinc(II) was synthesised according to the published procedure.[5]

The equilibrium constant for the complexation of [Zn(obtpp)] with the neutral bases was determined using an optical absorption method at 298 K. Toluene was used as the solvent. The concentration of [Zn(obtpp)] was maintained at 5 × 10^{-5} mol dm^{-3} while that of the bases was varied from 1 × 10^4 to 2 × 10^{-1} mol dm^{-3}. The value of K was evaluated from the

decrease or increase in absorbance of the Q transition of [Zn(obtpp)] on increasing addition of base. The solvation equilibria of [Zn(obtpp)] with dimethyl sulfoxide were also investigated in a similar manner.

The spectral measurements were carried out on instruments described elsewhere.[5]

Crystallography.—Single crystals of $[Zn(obtpp)(PrCN)_2]$ was obtained by slow evaporation of a $CHCl_3$–PrCN (3:1 v/v) solution of [Zn(obtpp)] at room temperature.

Crystal data. $C_{52}H_{34}Br_8N_6Zn$, M = 1459.4, triclinic, space group $P\bar{1}$, a = 14.252(4), b = 14.276(3), c = 14.308(4) Å, α = 115.82(3), β = 106.30(3), γ = 90.26(3)°, U = 2487.94 Å^3 (by least-squares refinement of 25 reflections), λ = 0.7107 Å, Z = 2, D_c = 1.948 g cm^{-3}, $F(000)$ = 1396. Dark brown tablets, crystal dimensions 0.3 × 0.2 × 0.2 mm, μ(Mo-Kα) 68.25 cm^{-1}.

Data collection and processing. A CAD4 diffractometer was employed with graphite-monochromated Mo-Kα radiation. A ω–2θ scan mode with scan width = 0.35 + 1.05 tan θ mm, ω scan speed = 1.28–5.53° min^{-1}. 8716 Reflections unique (merge R = 0.02); $1 < \theta < 25°$; $+h, \pm k, \pm l$); absorption correction (maximum, minimum transmission factors 0.96, 0.80); 3931 observed reflections [$F_o > 6.0\sigma(F_o)$].

Structure analysis. The Patterson heavy-atom method and successive Fourier difference syntheses were employed.[22] Full-matrix least-squares refinement with all non-hydrogen atoms anisotropic; weighting scheme $w = 2.1818/[\sigma^2(F_o) + 0.002\,183(F_o)^2]$ with $\sigma(F_o)$ from counting statistics. Final R = 0.080 and R' = 0.084.

Additional material available from the Cambridge Crystallographic Data Centre comprises thermal parameters and remaining bond lengths and angles.

Acknowledgements

The authors thank the Department of Science and Technology for financial support.

References

1 M. Gouterman in, *The Porphyrins*, ed. D. Dolphin, Academic Press, New York, 1978, vol. 3.
2 M. Nappa and J. S. Valentine, *J. Am. Chem. Soc.*, 1978, **100**, 5075.
3 O. W. Kooling, *Anal. Chem.*, 1982, **54**, 260.
4 R. M. Wang and B. M. Hoffmann, *J. Am. Chem. Soc.*, 1984, **106**, 4235.
5 P. Bhyrappa and V. Krishnan, *Inorg. Chem.*, 1991, **30**, 239.
6 J. R. Platt and H. B. Klevens, *Rev. Modern Phys.*, 1944, **16**, 182.
7 Y. Marcus, *Ion Solvation*, Wiley, New York, 1985; *J. Soln. Chem.*, 1984, **13**, 599; V. Gutmann, *Coord Chem. Rev.*, 1976, **18**, 225.
8 A. V. Hill, *J. Physiol. London*, 1910, 40, IV–VII; C. A. Hunter, M. N. Meah and J. K. M. Sanders, *J. Am. Chem. Soc.*, 1990, **112**, 5773.
9 J. R. Miller and G. D. Dorough, *J. Am. Chem. Soc.*, 1952, **74**, 1277.
10 J. B. Cooper, C. T. Brewer and G. A. Brewer, *Inorg. Chim. Acta*, 1987, **129**, 25.
11 G. C. Vogel and J. R. Stahlbush, *Inorg. Chem.*, 1977, **16**, 950.
12 C. H. Kirksey, P. Hambright and C. B. Storm, *Inorg. Chem.*, 1969, **8**, 2141.
13 C. K. Schauer, O. P. Anderson, S. S. Eaton and G. R. Eaton, *Inorg. Chem.*, 1985, **24**, 4082.
14 C. K. Johnson, ORTEP-II, A Program for thermal ellipsoid plotting, Oak Ridge National Laboratory, Oak Ridge, TN, 1976.
15 D. Mandon, P. Ochsenbein, J. Fischer, R. Weiss, K. Jayaraj, R. N. Austin, A. Gold, P. S. White, O. Brigand, P. Battioni and D. Mansuy, *Inorg. Chem.*, 1992, **31**, 2044.
16 K. M. Barkigia, M. D. Barber, J. Fajer, G. J. Medforth, M. W. Fenner and K. M. Smith, *J. Am. Chem. Soc.*, 1990, **112**, 8851.
17 E. B. Fleischer, C. K. Miller and L. E. Webb, *J. Am. Chem. Soc.*, 1964, **86**, 342; M. D. Glick, G. H. Cohen and J. L. Hoard, *J. Am. Chem. Soc.*, 1967, **89**, 1996; W. R. Scheidt, M. E. Kastner and K. Hatano, *Inorg. Chem.*, 1978, **17**, 706.
18 W. R. Scheidt and Y. Lee, *Struct. Bonding (Berlin)*, 1987, **64**, 1.
19 M. Gouterman, *J. Chem. Phys.*, 1959, **30**, 1139.
20 D. M. Collins and J. L. Hoard, *J. Am. Chem. Soc.*, 1970, **92**, 3761.
21 A. Giraudeau, M. Gross and H. J. Callot, *Electrochim. Acta*, 1981, **26**, 1839.
22 G. M. Sheldrick, SHELX 76, Program for crystal structure determinations, University of Cambridge, 1976.

Received 9th December 1992; *Paper* 2/06557F